Atmospheric Radar for the 0.5–110 km Region

Iain M. Reid
Department of Physics and Mathematical Physics
The University of Adelaide, Adelaide, Australia, 5005

***Abstract*—Radar can be used to make measurements of the dynamics and structure of the atmosphere by detecting irregularities in refractive index due to variations in humidity and temperature in the lower atmosphere (0 – 20 km), and due to variations due to fluctuations in electron density in the Mesosphere Lower Thermosphere (MLT) region of the upper atmosphere (50 – 110 km). MF and HF radars have been used to routinely investigate the MLT for over 50 years. Wind Profiling Radars operating in the VHF band have been used for about 25 years to investigate the Stratosphere Troposphere (ST) region, but only routinely in the last 15 years. Considerable development has occurred within the past decade. In particular, great attention has been paid to interferometric and imaging techniques, to a re-examination and extension of MF radar techniques, to the application of VHF radars developed for atmospheric research to meteor studies, and finally, a rebirth of dedicated meteor radars has occurred. Here we briefly describe some of these recent improvements.**

I. Introduction

Most atmospheric radars operate in a monostatic configuration in a pulsed mode and utilize backscatter from irregularities in the refractive index of the atmosphere. Operating frequencies range from around 2 to 1000 MHz, with the higher frequencies being utilized for observations in the lowest part of the atmosphere. Some of the various types are summarized in Table 1 below. The diurnal variation in performance for MLT radars reflects the solar control of the ionization of the 60 to 80 km height region, and the consequent availability of free electrons to act as tracers for the neutral motions.

TABLE I
TYPES OF ATMOSPHERIC RADAR

Type	Frequency	Winds
MF Partial Reflection Radars	2 – 3 MHz	~60 – 100 km (day) ~80—100 km (night)
Meteor Radars	30 – 50 MHz	80 – 100 km
Mesosphere Stratospheric Tropospheric (MST) Radars	45 – 65 MHz	1 – 20 km 60 – 80 km (day)
Stratospheric Tropospheric Radars	45 – 65 MHz	1 – 20 km
	400 – 490 MHz	0.5 – 18 km
Boundary Layer Troposphere (BLT) Radars	45 – 65 MHz	0.2 – 8 km
Boundary Layer (BL) Radar	915 – 1300 MHz	0.1 – 3 km

There are three main mechanisms believed to result in the return of radio waves from irregularities in the atmosphere. These are scattering from turbulence ("Turbulent" Scatter), Fresnel Reflection or Fresnel Scatter, and Thermal Scatter. Thermal (also known as Incoherent or Thomson) will not be discussed further here (for reviews see [1] and [2]). Turbulent (or Bragg) scatter results from the production of irregularities in refractive index by turbulence, for which the dominant Fourier scales correspond to half the projection of the wavelength of the radar onto the radiowave vector. Fresnel reflection (also known as partial reflection) results from the presence of irregularities in refractive index transverse to the radio wave propagation direction that are thin compared to the radar wavelength. For vertical incidence, true Fresnel reflection requires that the horizontal extent of the irregularity be greater than one Fresnel zone, which is $(\lambda z)^{1/2}$, where λ is the wavelength and z the height of scatter, and that the vertical extent of the irregularity be less than about $\lambda/4$. In practice, the minimum horizontal extent of the irregularity needs only be greater than that of the radar beam, and steps in refractive index of vertical extent less than $\lambda/4$ will often contain Fourier scales strong enough to produce radar returns. Fresnel scatter results when the scattering medium is coherent in the two dimensions transverse to the probing wave, and random in the direction parallel to the radiowave vector. A more complete discussion of the various scattering mechanisms is given in [3].

With practical observations, it is often not easy to determine which mechanism dominates, and a major uncertainty in the nature of the scattering concerns whether radar returns occur from true steps in refractive index, that is, partial reflection, or from turbulent scatter from anisotropic irregularities (see e.g., [4]). A basic problem is that sharp gradients persist for much longer than is expected given the mixing and diffusive processes that occur in the atmosphere. For example, at mesospheric heights, sharp gradients should be rapidly weakened through molecular diffusion. One notion due to Bogliano [5] combines the two scattering mechanisms and may provide a partial explanation. He suggested that turbulent regions would be bounded by sharp gradients in electron density, and that partial reflection might occur from these boundaries.

Atmospheric radars use the gradients in the refractive index as targets to determine the motion of the background wind and turbulence intensity using a variety of techniques. The refractive index, n, of air at frequencies greater than around 30 MHz is given by

$$n = 1 - 0.373\frac{e}{T^2} + 77.6\times10^6\frac{p}{T} - 40.3\frac{N_e}{f^2}, \qquad (1)$$

where e is the humidity, T the temperature, p the pressure, N_e the electron density and f the frequency. Fluctuations in e, T and N_e with a scale the order of half a wavelength produce Bragg scatter. Discontinuities in refractive index of the order of less than a tenth of a wavelength also act as targets.

The second two terms in equation (1) refer to fluctuations in the neutral atmosphere, with the humidity term dominating at heights below around 5 km. The last term refers to fluctuations in electron density in the ionosphere, and is important at heights above around 50 km.

The nature of the irregularities themselves is not well understood. There are two limiting cases, scatter from isotropic turbulence and scatter from a single, sharply bonded discontinuity. The power P_R returned in the case of isotropic turbulence when volume scatter occurs is given by

$$P_R = \frac{\pi P A \alpha \Delta R}{64 R^2} \eta, \tag{2}$$

where P is the transmitted power, A is the effective antenna area, α is the total efficiency factor of the system, ΔR the radar pulse length range, R the range, and η the volume reflection coefficient, a measure of the strength of the turbulence.

Scatter also occurs from sharp steps or gradients in refractive index. In this case, the scatter is termed Fresnel scatter or Fresnel reflection. The power returned is given by

$$P_R = \frac{P A^2 \alpha}{4 \lambda^2 R^2} |\rho|^2, \tag{3}$$

where λ is the radar wavelength, and ρ is the amplitude reflection coefficient. The presence of relatively long-lived sharply bounded gradients in refractive index that should be rapidly dissipated by turbulent and diffusive effects, and which are readily detected by both high resolution balloon soundings and radars is a particularly poorly understood aspect of the atmosphere.

Radar returns from the atmospheric at frequencies lower than UHF usually consist of a mixture of both Bragg and Fresnel types of scatter, and exhibit considerable aspect sensitivity, with maximum returns from the zenith.

The performance of an atmospheric radar system can be roughly described by the product of P and A, the "power aperture product" that appears in equations (2) and (3). Generally, at VHF, a power aperture product exceeding around 5 x 10^7 Wm^2 would provide a measurement capability throughout the 1 to 20 Km height region, and provide a limited daytime mesospheric (60 – 80 km) measurement capability. Most current VHF radars utilize the Doppler Beam Swinging (DBS) Technique.

II. Doppler Techniques

A. Doppler Beam Swinging (DBS) Technique

When cost is not the major concern, the formation of multiple narrow Doppler beams to measure radial velocities, and the recombination of these velocities to construct the total wind field, is arguably the optimum configuration. The DBS technique provides the greatest control over experimental design, and has fewer ambiguities and uncertainties than other techniques. However, like all techniques, it is better suited to some investigations of atmospheric dynamics and structure than others. Some aspects of its limitations are discussed in Reid [6], and an interesting comparison of the Doppler and spaced sensor techniques is given by May [7]. Most Doppler radars now utilize a symmetric five-beam arrangement rather than the previously common three-beam arrangement to permit the determination of additional parameters including the density normalized upward flux of horizontal momentum [8]. An example of a state of the art atmospheric Doppler radar is described in Figure 1.

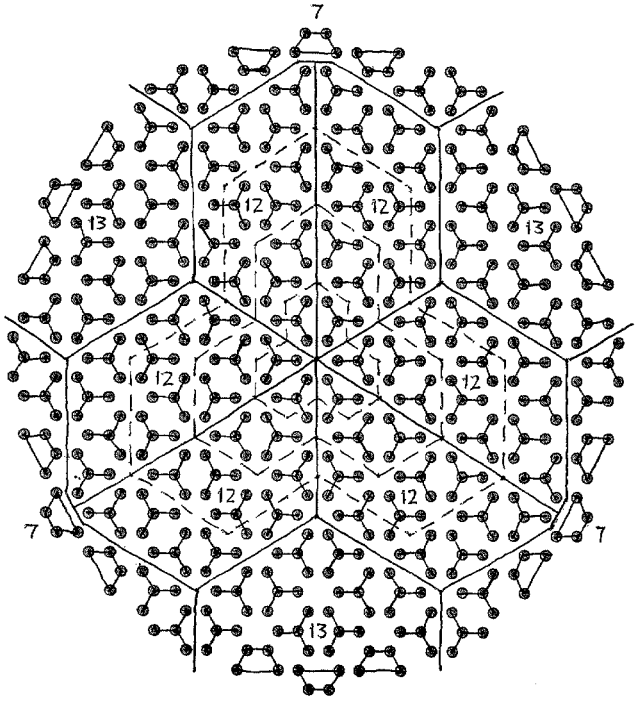

Figure 1: The antenna layout for the VHF (54 MHz) phased array radar currently under construction in Wuhan, China. This system consists of 512 three-element Yagi antennas, each of which is driven by a 1 kW solid-state power amplifier, and typifies a state of the art system. Each Power Amplifier (PA) can be amplitude controlled, and phase controlled to within 1°. The array is about 100-m in diameter with a power aperture product of about 2×10^8 Wm^2. Antenna spacings are less than a wavelength in any direction, permitting beam formation in any azimuthal direction without grating lobes. The PA's are distributed within the antenna field, greatly reducing cable losses.

B. Hybrid Doppler Interferometer

A major consideration with radars operating in the lower VHF band is the effect of the atmospheric aspect sensitivity on the antenna polar diagrams. For the DBS technique, with off-vertical beams, the effect is to bias the polar diagrams back towards the zenith. With relatively broad beams (or relatively small antenna arrays, say > 4°) the effect can result in severe underestimation of the radial velocities.

However, if the mean angle of arrival can be determined, the bias can be determined. This suggests a combined Doppler – Interferometer mode of operation, in which hardware beam-steering is applied on transmission to form a relatively narrow transmit beam, and the returned signal is received on multiple sections of the array, so that the receive beam can be formed in software (see Figure 2).

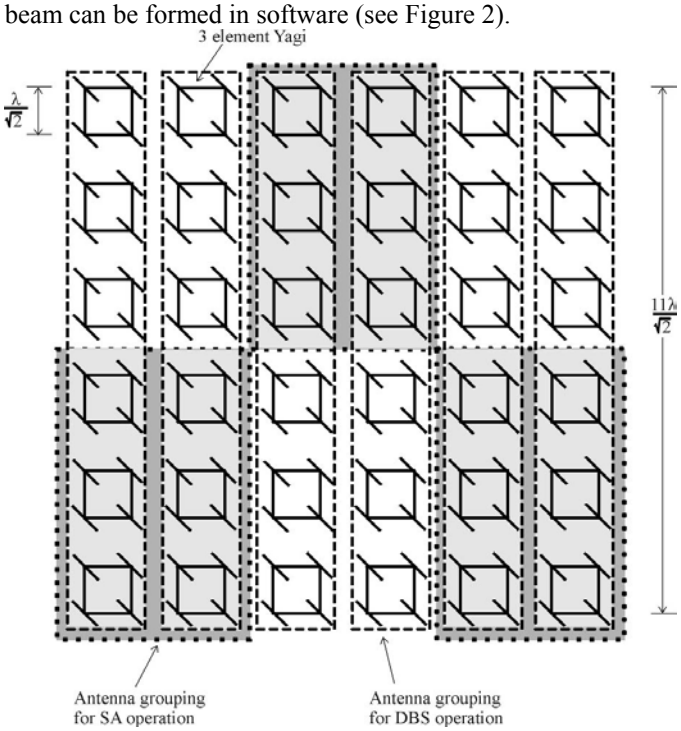

Figure 2: Antenna layout for the Davis Station VHF (55 MHz) Radar. The system can be configured to operate as a Doppler radar when the six rows (or columns) are used to form a beam, or as a Spaced antenna radar, when three sub-groups, such as the three shaded sub-sections are used.

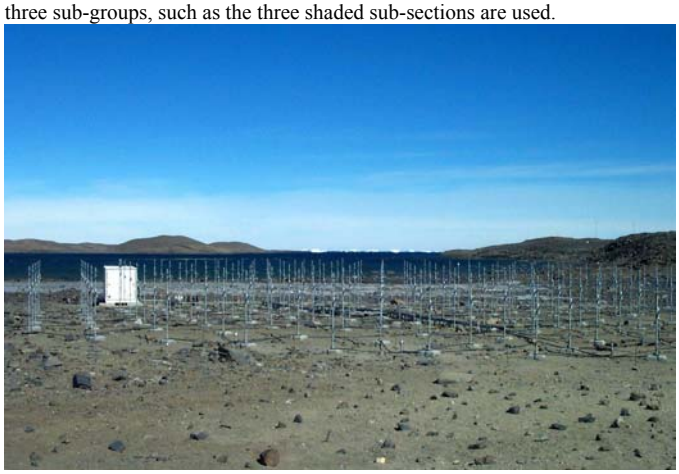

Figure 3: Photograph of Davis Station VHF radar, showing the antenna layout and equipment building (photo courtesy of Damian Murphy, Australian Antarctic Division). The PA product of this system will be about 1×10^7 Wm^2 when completed.

C. *Non-Filled Arrays*

Recently, new arrays similar to that operated at Bribie Island in Queensland for some years [9] have been constructed at both HF and VHF [10]. These typically consist of two orthogonal arms of antennas, each of which produces a fan type polar diagram. In earlier systems, one arm was used for transmission, and the other for reception, but most new systems transmit and receive on both arms. The intersection of these fan beams is a pencil type beam, which can be utilized for Doppler work. The advantage of such arrays is that fewer antennas are required to achieve a relatively narrow beam. The disadvantage is that not all of the transmitted power is available in the receive beam, and sidelobes may limit performance. Such arrays are particularly attractive for work at MF in the MLT region, where the radar backscatter cross-section is very high, and the antenna arrays for Doppler work are necessarily very large physically. An example of one antenna layout used with this type of system is shown in Figure 4.

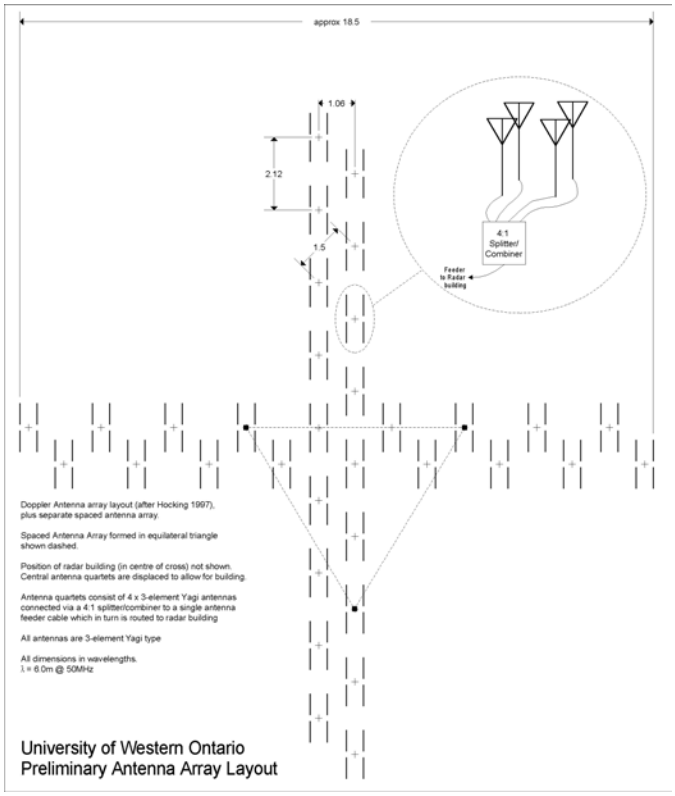

Figure 4: A non-filled VHF antenna array based on the layout used by [10] (diagram courtesy of Atmospheric Radar Systems Pty Ltd).

III. Spaced Antenna Techniques

In many situations, the Spaced Antenna (SA) technique utilizing the Full Correlation Analysis (FCA) offers advantages. These include the need for only relatively small antenna arrays, and no requirement for beam steering.

The DBS and SA methods use the same information. The DBS technique exploits the change in the mean Doppler shift with azimuth angle, and samples small spatially separated volumes. The SA methods make use of the fact that the variation in the Doppler shift with angle is such that the resultant field moves over the ground as a random pattern with a velocity twice that of the horizontal wind at the backscatter height (see [11]). The advantage of these techniques is that small antenna arrays can be used, because only broad, vertically directed beams are required. These techniques are all variations on imaging techniques in the sense that they attempt to reconstruct the ground diffraction pattern produced by backscatter from irregularities in refractive index, and so infer the backscatter polar diagram from a limited set of observations on the ground. Most recently, cheaper and faster computing has permitted a

larger number of receiver channels to be economically employed to sample the ground diffraction pattern.

For the SA technique, the aspect sensitivity of the atmosphere results in a narrowing of the vertically directed beam pattern, and this generally has no adverse effect on the technique. There are several variants of the technique that utilize various antenna arrangements, which result in the same basic data, but which are analyzed in different ways. The most common are the Full Correlation Analysis (FCA), and the Imaging Doppler Interferometer (IDI) techniques.

Figure 5: Photo of the Sydney Airport BLT radar system. This system operates near 54 MHz with a peak power of 7.5 kW. The array consists of three groups of nine three-element yagi antennas and the system has a PA product of 3.5×10^4 Wm^2.

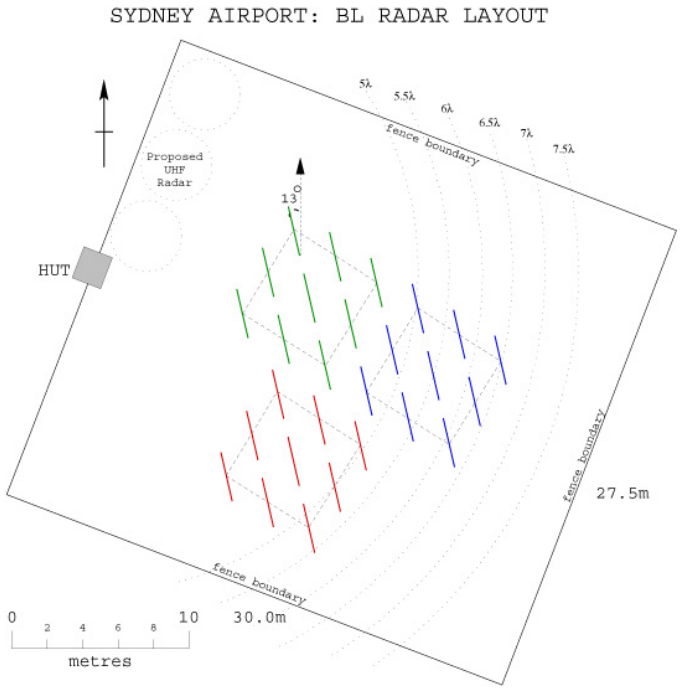

Figure 6: Antenna layout of the Sydney Airport BLT radar system. Data from the three antenna sub-groups are used with the FCA analysis to yield horizontal wind velocities in the 0.3 to 6 km height region. The acceptance fraction refers to the number of valid one minute wind determinations in each hour.

A. The FCA Technique

This spaced-sensor technique has been applied at MF to investigate the atmosphere in the 60-100 km height region since the mid-1960's [12], and has been applied at VHF to measure wind velocities in the 2-20 km height region since the mid-1970's [13]. It has also been applied at VHF to mesospheric data [14]. It has most recently been exploited in the development of small Boundary Layer Tropospheric (BLT) radars operating at frequencies near 50 MHz [15] to measure wind velocities in the 0.2 to 6 km height region. This has required the development of faster T/R switches than normally used at this frequency. An example of this radar type is shown in Figure 5. This system is installed at Sydney Airport and is operated by the Australian Bureau of Meteorology.

The technique utilizes a minimum of three spaced antennas to sample the ground diffraction pattern produced by the backscattering irregularities, and cross correlation techniques are used to determine its velocity of motion. The analysis takes account of random changes in the pattern, and also any anisotropy of the pattern, so that both horizontal components of the wind field are measured at a particular height in a single region directly above the radar. The analysis itself is termed the Full Correlation Analysis (FCA) (see [16]).

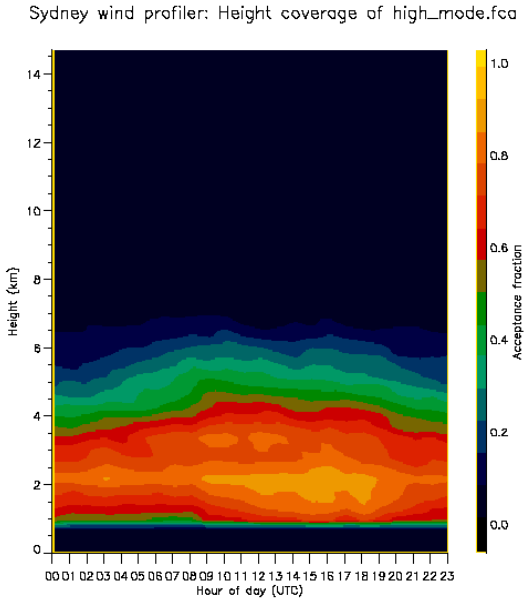

Figure 7: Height coverage of wind velocity measurements from the Sydney Profiler for a two-month period in high mode. In low-mode the system delivers results from 0.3 km upwards. The acceptance fraction refers to the number of one minute observations in each hour which result in a valid wind determination.

B. IDI-Like Techniques

One of the first of a group of new interferometric techniques was termed Imaging Doppler Interferometry (IDI) [17]. The aim of this technique is to track individual radiowave scatterers in the neutral atmosphere, and it was first applied at Medium Frequencies (MF). The experimental setup utilizes spaced antennas to sample the radio waves partially reflected or backscattered from the atmosphere. The analysis then looks for evidence of down-coming plane wave radiation, and uses spectral techniques to locate a scattering position for each frequency bin. A radial velocity is associated with each scattering position and the entire wind field can then be reconstructed.

The raw data acquired by the IDI and other SA techniques are essentially identical. The techniques differ in the

assumptions they make about the backscattering medium, and consequently, in the subsequent analysis. IDI-like techniques assume that discrete scattering regions exist in the atmosphere. The other non-IDI SA techniques assume volume scatter. However, modeling studies suggest that there is no theoretical reason for the FCA not to work well when backscatter is from more than about ten discrete irregularities moving with the background wind [18], [19].

IDI-like techniques make no allowance for the presence of random changes in the backscatter produced by, for example, turbulence. Vandepeer and Reid [20] have shown theoretically that IDI-like techniques measure what is termed the "apparent" velocity in the FCA technique in the case of volume scatter. This is the velocity inferred when random changes and pattern anisotropy are not taken into account. It has values considerably larger than those of the actual wind velocity. Vandepeer and Reid also presented experimental results, which partially supported their theoretical result. In spite of these concerns, the technique appears to yield very usable results when appropriate care is taken [21], and it has also been applied to digital ionosonde type radars [22] where the results suggest that the wind directions are in good agreement with other techniques, but with the wind magnitudes somewhat overestimated.

IV. Temperatures and Electron Densities from Radar Observations

A. Differential Absorption / Differential Phase Experiment at MF

The DAE and DPE techniques are old methods suitable for use at MF and HF (see e.g., [23], [24]) in the MLT region. They provide a coarse measure of the electron density, but relative changes in electron density can be closely monitored. The technique relies on the fact that the ionosphere is birefringent, so that the relative strengths of the ordinary and extra-ordinary modes of radiowaves partially reflected from the region vary. These modes correspond to left and right-handed circular polarization with respect to the Earth's magnetic field direction, respectively. Not utilized for some years, these techniques have been revived and are presently being successfully applied on new MF radars [25], [26].

B. Temperatures and Electron Densities from Meteor Observations

Temperatures have been determined from the ambipolar diffusion constant determined from the decay of meteor trails detected with VHF radar [27], [28], [29]. This technique may also have potential at MF/HF because work by Olsson-Steel and Elford [30], [31], [32] has suggested a substantial flux of meteors detectable at 2 and 6 MHz in this region. Another development is the measurement of electron densities using Faraday rotation of radar meteor returns at VHF [33]. This technique appears to be promising for narrow beam meteor radars, where the differential rotation of the electric field from meteors detected at different heights in the narrow beam can be used to infer the electron density between those heights, but is more difficult to apply routinely to all-sky systems.

C. Dedicated All-Sky Meteor Systems

All-sky meteor systems using an interferometric receiving arrangement have been developed to measure winds in the 80 to 100 km height region. Operating in the range 30 to 55 MHz, count rates of the order of 9–10,000 unambiguous meteor detections per day are typical. Examples typical of these systems are shown in Figures 8 to 10. Figure 8 shows meteor detections in sky-map form over a 24 h period over Adelaide. After a meteor trail is formed, it drifts with the background wind. At this time, the phase of the meteor echo corresponds to the radial velocity of this drift with the background wind. With sufficient trail detections, the entire wind field may be determined.

Figure 9 shows the decay times and diffusion coefficients of each of the trails as a function of height. These are used together with a standard atmosphere to determine the temperature and temperature perturbations as a function of height and time. Figure 10 shows the wind velocities derived from the detections shown in Figure 8 as a height time plot. These observations show the rotation of the wind field as a function of height and of time associated with atmospheric tides.

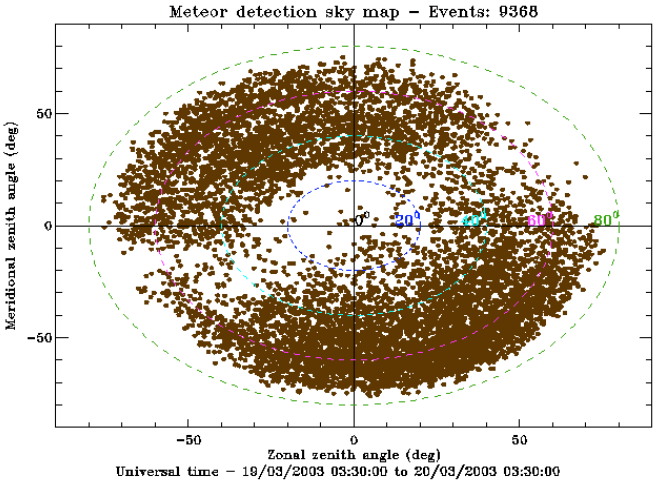

Figure 8: Sky map showing the meteor detections over one 24-h period over Adelaide at 31 MHz.

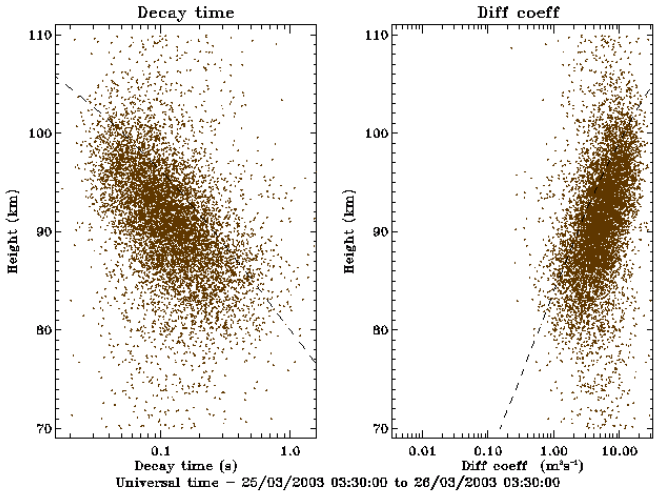

Figure 9: Meteor trail decay times (left) and diffusion coefficients derived from them for a 24 h period over Adelaide. Note the fact that detections occur largely between 80 and 100 km.

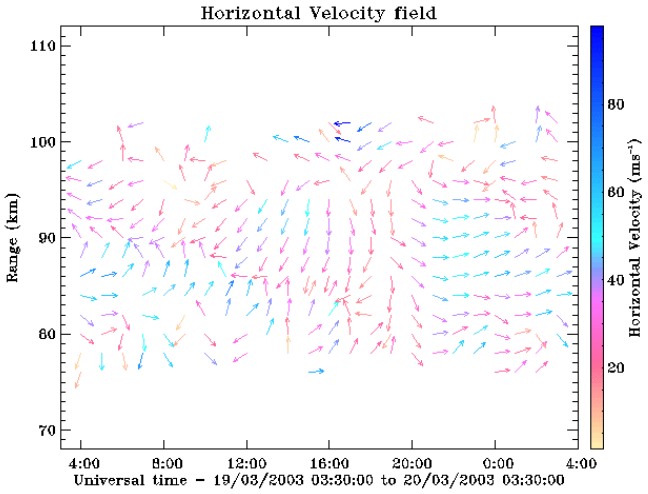

Figure 10: Wind velocities derived from the meteor detections shown in Figure 8.

D. Extension of MF/HF Radar Height Coverage

Work on the correction of MF meteor data for the effects of initial radius and diffusion suggest no evidence for reduction in flux up to around 140 km where the trails begin to ionise the atmosphere [34]. This implies a population of low ablation temperature particles of CHON composition. This raises the potential of measuring drifts and thus the wind fields in the region (whilst noting the gross effect of the magnetic field), and also the potential to measure the incoming velocities of meteoroids [35]. Meteors detected at 2 MHz have been used to determine winds in the MLT region [36], but the technique is complicated by the presence of ionospheric echoes. Particularly good results have been obtained by Tsutsumi at high southern latitudes during winter, when the contamination from ionospheric echoes is reduced. The implementation of pulse coding may improve the coverage in the lower height ranges, and this scheme is now being implemented on new MF radars. Further capabilities of MF/HF radars are reviewed with particular reference to the Buckland Park MF radar in [21]. Recently, useful meteor wind observations have been obtained from the SuperDARN class (see e.g., [37]) of HF radar [38]

E. Fresnel Techniques

Radiowave diffraction from a meteor trail is Fresnel in nature. Applying a Fresnel transform to the amplitude and phase of the return from the ionized trail produced by the meteor extends the information available. This includes application to both under- and over- dense trails, and to meteor head echoes, application to the determination of meteoroid speeds; and the ability to identify multiple sources and thus fragmentation processes [39].

V. Conclusion

This paper has provided a brief overview of atmospheric radars operating from the MF to lower VHF band used to investigate the atmosphere up to heights of around 110 km. More detailed descriptions of the capabilities of MF/HF radar systems are provided in [21], of the meteorological applications of VHF radar systems in [40], and of HF ionospheric radar applications in [37].

Acknowledgment

Contributions to the development of the radars and analysis techniques described in this paper by D. A. Holdsworth, R. A. Vincent, W. G. Elford, R. J. Morris, D. J. Murphy and by the staff of Atmospheric Radar Systems Pty Ltd are gratefully acknowledged. Useful comments from two anonymous referees are appreciated.

References

[1] R. M. Harper and W. E. Gordon, *Radio Sci.,* 15, 195, 1980.
[2] J. D. Mathews, in: *Handbook for MAP,* 13, ed R. A. Vincent, SCOSTEP Secretariat, University of Illinois, Urbana,135,1984.
[3] K. S. Gage and B. B. Balsley, *Radio Sci.,* 15, 243, 1980.
[4] W. K. Hocking, *Adv. Space Res.,* 7,327,1987.
[5] R. Bogliano, in *Winds and Turbulence in Stratosphere, Mesosphere and Ionosphere,* ed. K. Rawer, North- Holland, Amsterdam, 371, 1968.
[6] Reid *et al*, *J. atmos. terr. Phys., 49*, 467-484, 1987.
[7] May, P. T., *Radio Sci*., 25, 1111, 1990.
[8] Vincent, R.A. and I.M. Reid, *J. atmos. Sci*., 1983.
[9] From, W. R. and J. D. Whitehead, *Radio Sci*., 19, 423, 1983.
[10] Hocking, W.K., *Radio Sci.,* 32, 687-706, 1997
[11] Briggs, B. H., *J atmos. terr. Physics*, 42, 823, 1980.
[12] Fraser, G., *J Atmos. Sci.,* 22, 217, 1965.
[13] Vincent R. A. and J. Roettger, *Radio Sci.,* 15, 319, 1980
[14] Chilson, P. B., T.-Y. Yu, R. D. Palmer, and S. Kirkwood, Annales Geophysicae, 20, 213–223, 2002
[15] Vincent, R.A., *et al., Radio Sci.,* 33, 845-860, 1998.
[16] Briggs, B. H., SCOSTEP Secretariat, *Handbook for Map*, 13, 166, 1984
[17] Adams, W. and J. W. Brosnahan, D. C. Walden and S. F. Nerney, *J. Geophys. Res*., 91, 1671, 1986.
[18] Holdsworth, D. A., and I. M. Reid, *Radio Sci*., 30, 1263-1280, 1995a.
[19] Holdsworth, D. A. and I. M. Reid, *Radio Sci*., 30, 1417-1433, 1995b.
[20] Vandepeer, B. G. W., and I. M. Reid, *Radio Sci*., 30, 885, 1995a.
[21] Holdsworth, D.A., I. M. Reid, R. Vuthaluru and R. A. Vincent, Mesospheric and lower thermospheric observations using the Buckland Park medium frequency radar, this volume, 2003
[22] Jones, G. O. L., and C. J. Davis, *J. Atmos. Sol. Terr. Phys.,* 60, 595, 1998
[23] Belrose, J.S., *J. atmos. terr. Phys*., 32, 567, 1970.
[24] Manson, A.H. and C.E. Meek, *Handbook for MAP,* 13, SCOSTEP Secretariat, 113, 1984.
[25] Holdsworth, D.A., R. Vuthaluru, I. M. Reid and R. A. Vincent, *J. Atmos. Solar Terr. Phys*, 64, 2029 – 2042, 2002.
[26] Vuthaluru, R., R.A. Vincent, D.A. Holdsworth, and I.M. Reid, *J. Atmos. Solar Terr. Phys*, 64, 2043 – 2054, 2002
[27] Tsutsumi, M., T. Tsuda, T. Nakamura, and S. Fukao, *Radio Sci*., 29, 599-610, 1994.
[28] Nakamura, T., T. Tsuda, S. Fukao, H. Takahashi, P. P. Batista, and R. A. Buriti, *Handbook for STEP*, pp92-95, July 1996.
[29] Cervera, M. A. and I. M. Reid, Radio Sci., 35, 833, 2000.
[30] Olsson-Steel, D.I. and W.G. Elford, *J. Atmos. Terr. Phys*., 49, 243, 1987.
[31] Olsson-Steel, D.I. and W.G. Elford, *J. Atmos. Terr. Phys.*, 50, 811, 1988.
[32] Steel, D.I. and W.G. Elford, *J. atmos. terr. Phys*., 53, 409, 1991.
[33] Elford, W.G. and Taylor, A. D., *J. atmos. terr. Phys*., 59, 1021, 1997.
[34] Grant, S.G. and W.G. Elford, *private communication*, 2003.
[35] Taylor, A. D., Cervera, M.A., Elford, W.G. and Steel, D.I.., Proc. IAU Colloq. 150, *Physics, Chemistry, and Dynamics of Interplanetary Dust*, eds. B. Gustofson and M. Hammer, Astronomical Society of the Pacific, San Francisco. 104, IAU, ASP Conf. Ser.,75-78, 1997.
[36] Tsutsumi, M., D. A. Holdsworth, T. Nakamura, and I. M. Reid, *Earth, Planets and Space,* 51, 691-700, 1999.
[37] Dyson, P.L., J. C. Devin, M. L. Parkinson, J. S. Whittington, The Tasman International Geospace Environment Radar (TIGER) – Current Development and Future Plans, this volume, 2003.
[38] Yukimatu, A.S., and M. Tsutsumi, *Geophys. Res. Lett.,* 29, 2002.
[39] Elford, W.G., in *Meteoroids 2001: Conference at the Swedish IRF*, European Space Agency, 405, 2001.
[40] Lucas, C., Meteorological Applications of Radar Wind Profilers, this volume, 2003.